

Article

Effects of Polymerization Time towards Conductivity and Properties of Poly(methyl methacrylate)/Polyaniline (PMMA/PANi) Copolymer

Helyati Abu Hassan Shaari^{1,2}, Muhammad Mahyiddin Ramli^{3,*}, Mohd Mustafa Al Bakri Abdullah³, Mohd Nazim Mohtar^{1,3,4,*}, Norizah Abdul Rahman^{1,5}, Azizan Ahmad^{6,7}, Nurul Huda Osman^{3,8} and Febdian Rusydi⁷

- ¹ Institute of Nanoscience and Nanotechnology, Universiti Putra Malaysia, Serdang 43400, Selangor, Malaysia; helyati87@gmail.com (H.A.H.S.); a_norizah@upm.edu.my (N.A.R.)
- ² Faculty of Applied Sciences, Universiti Teknologi MARA Perlis Branch, Arau Campus, Arau 02600, Perlis, Malaysia
- ³ Centre of Excellence Geopolymer and Green Technology (CEGeoGTech), Universiti Malaysia Perlis (UniMAP), Kangar 01000, Perlis, Malaysia; mustafa_albakri@unimap.edu.my (M.M.A.B.A.); nurulhuda@upm.edu.my (N.H.O.)
- ⁴ Faculty of Engineering, Universiti Putra Malaysia, Serdang 43400, Selangor, Malaysia
- ⁵ Department of Chemistry, Faculty of Science, Universiti Putra Malaysia, Serdang 43400, Selangor, Malaysia
- ⁶ Department of Chemical Sciences, Faculty of Science and Technology, Universiti Kebangsaan Malaysia, Bangi 43600, Selangor, Malaysia; azizan@ukm.edu.my
- ⁷ Department of Physics, Faculty of Science and Technology, Universitas Airlangga, Jl. Mulyorejo, Surabaya 60115, Indonesia; rusydi@fst.unair.ac.id
- ⁸ Applied Electromagnetic Laboratory 1, Department of Physics, Faculty of Science, Universiti Putra Malaysia, Serdang 43400, Selangor, Malaysia
- * Correspondence: mmahyiddin@unimap.edu.my (M.M.R.); nazim@upm.edu.my (M.N.M.)



Citation: Abu Hassan Shaari, H.; Ramli, M.M.; Abdullah, M.M.A.B.; Mohtar, M.N.; Abdul Rahman, N.; Ahmad, A.; Osman, N.H.; Rusydi, F. Effects of Polymerization Time towards Conductivity and Properties of Poly(methyl methacrylate)/Polyaniline (PMMA/PANi) Copolymer. *Sustainability* **2022**, *14*, 8940. <https://doi.org/10.3390/su14148940>

Academic Editor: Anastasia V. Penkova

Received: 20 June 2022

Accepted: 19 July 2022

Published: 21 July 2022

Publisher's Note: MDPI stays neutral with regard to jurisdictional claims in published maps and institutional affiliations.



Copyright: © 2022 by the authors. Licensee MDPI, Basel, Switzerland. This article is an open access article distributed under the terms and conditions of the Creative Commons Attribution (CC BY) license (<https://creativecommons.org/licenses/by/4.0/>).

Abstract: The effects of various polymerization times on the properties and conductivity of poly(methyl methacrylate)/polyaniline (PMMA/PANi) copolymer has been investigated. Different polymerization times, such as 1 h, 2 h, and 3 h, have been employed during free radical copolymerization of PMMA/PANi copolymer. The properties of newly synthesized PMMA/PANi copolymer were discussed with the help of Fourier transform infrared (FTIR), ¹H nuclear magnetic resonance (NMR) spectroscopies, UV-Vis spectroscopy, and transmission electron microscopy. All copolymers showed electrical conductivity of a semi-conductor material, compared with PMMA itself. It was found that the reaction played a significant role, especially at optimum polymerization time, where PANi formation and conductivity was at its highest. Our present work demonstrates that copolymer film could be a promising material to fabricate polymer conducting film in many electronics applications.

Keywords: poly(methyl methacrylate); polyaniline; copolymer; free-radical; conductivity

1. Introduction

Since the discovery of conducting polyacetylene in the year 1974 by Hideki Shirakawa, Alan Heeger, and Alan MacDiarmid [1], conducting polymers have been the main subject of interest for many researchers. The vast interest is due to their outstanding unique characteristics, including high optical and mechanical properties, flexibility in electrical properties, ease of fabrication, and better environmental stability. Because of these properties, conducting materials could be extensively useful in electrical, electronics, and optoelectronics applications. Among various types of conducting polymers, polyaniline (PANi) is one of the most favorable materials being studied due to its combination properties of high conductivity by doping, simple processing at low cost, and better stability [2,3]. Nevertheless, poor solubility and processability of neat PANi, together with susceptibility to degrade

at high temperature results in poor mechanical strength that limits application [4,5]. To overcome these limitations, PANi is usually copolymerized with other insulating polymers to produce synergetic effects of newly polymerized conducting composite materials.

There are various polymers that can be used for fabricating conducting composites. Examples of thermoplastics that is usually used with PANi include polystyrene (PS) [6], poly (lactic acid) (PLA) [7], poly (vinyl alcohol) (PVA) [8], and poly (methyl methacrylate) (PMMA) [9–11]. Two different methods can be employed to produce composites of these monomers, namely polymer blends and copolymerization. Polymer blends involve physical mixing and the solvent casting method, while copolymerization can be carried out by either electrochemical or chemical polymerization. Among all these methods, copolymerization via free radical polymerization is of interest due to the high reactivity, high conversion, and mild reaction conditions [12]. Copolymerization via free radical polymerization was used as a polymerization reaction as it requires simple and low-cost production process, it is easy to set up, and has wide range of monomers. In addition, free radical polymerization requires less removal of moisture either being carried out in bulk phase or solution [13].

Copolymerization of a polymer is often carried out by chemical/electrochemical oxidation or reduction of different monomers to yield a copolymer in various forms, such as powders, thin films, colloids, and thin films, depending on the reaction conditions and applications of the copolymers. Among all the polymerization methods, chemical oxidation reaction is an advantageous method in copolymerizing PANi with other thermoplastic polymers due to the ease of synthesis of different functional polymers [14]. For PANi synthesis itself, various polymerization conditions, such doping concentrations, types of oxidants, polymerization temperature, and time, have been proven to affect not only PANi morphology and molecular weight, but also the yield and conductivity of PANi. The effects of these parameters have been discussed in the previous work [7,15–18], however, there is not much information on the effects of these parameters on PANi copolymers.

The main objective of this work is to fabricate a conducting material by copolymerizing PMMA with PANi. The synthesis of PMMA with PANi was carried out by free-radical polymerization reaction, with different polymerization times, keeping the other polymerization parameters constant. In this work, the effects of polymerization time on chemical bonding, morphology, as well as conductivities, have been studied. It has been reported that increasing the polymerization time resulted in an increment in PANi yield and particle size [19]. Too long polymerization time also was also reported to cause excessive oxidation of PANi and hence, causing degradation of PANi chain [20]. Thus, the results reported in this study in relation to polymerization time may contribute to the optimization of the synthesis process.

2. Materials and Methods

2.1. Materials

Methyl methacrylate (MMA) (99.5%), aniline (99.9%), benzoyl peroxide (BPO), and ammonium persulfate (APS) (98%) were obtained from Sigma Aldrich, Malaysia and used as monomer, initiator, and oxidant. Hydrochloric acid (HCl) was acquired from R&M Chemicals, Malaysia and diluted to 1.5 M before being used to dope aniline. Toluene (99.5%), analytical reagent (AR) grade methanol (99.9%) and chloroform were obtained from Merck. Deionized water (DIW) and distilled water were used for dilution and washing during the synthesis process. All chemicals except aniline used in this study were directly used without undergoing a purification process.

2.2. Free-Radical Polymerization of PMMA/PANi Copolymer

PMMA/PANi copolymer was synthesized by a free-radical polymerization reaction. The entire reaction was done under oxygen-free conditions by a flow of nitrogen gas. We used 0.1:0.0004 ratio of methyl methacrylate (MMA) monomer to benzoyl peroxide (BPO) initiator throughout this study. In a typical procedure, BPO was introduced into a

reaction flask containing 10 mL of MMA under stirring conditions at 60 °C polymerization temperature. Prior to the addition of BPO, the polymerization was allowed to start until gelation occurred, indicating that polymerization reaction had started. After a certain time, the solution became viscous, and a certain amount of toluene was added to the reaction to prevent coagulation of the polymer when the second monomer was added. Then, the second monomer, 1.5 M HCl doped aniline, was added slowly to the reaction. The ratio of the MMA to aniline monomer used was 1:3. After that, the polymerization temperature was reduced and the polymer mixture was left to copolymerize for different polymerization times, namely 1 h, 2 h, and 3 h. After the reaction reached the required polymerization time, methanol was added to stop the polymerization reaction. This step was followed by the washing process using an excess amount of methanol and distilled water three times to remove any impurities and un-reacted monomer. Then, the copolymer precipitate was collected and dried in an oven for 24 h. The precipitates collected at different polymerization times in this reaction are regarded as PMMA/PANi copolymers and labeled as PMMA/PANi 1, PMMA/PANi 2, and PMMA/PANi 3, respectively.

2.3. Preparation of PMMA/PANi Film

We dissolved 0.2 g of PMMA/PANi precipitate in chloroform (10 *w/v*%). Using a solvent casting technique, the dispersion was cast into a glass slide and left dry in an oven for 24 h at 60 °C to eliminate any leftover solvent from the film. This technique produces PMMA/PANi films with an average thickness of 0.08 mm.

2.4. Characterization

All samples were characterized by Nicolet 6700 FTIR (Thermo Scientific, Waltham, MA, USA) spectrometer. Infrared spectra were recorded at room temperature in a spectral range of 4000 to 500 cm^{-1} wave numbers.

The components present in the PMMA/PANi copolymer prepared were identified using proton nuclear magnetic NMR (^1H NMR), using deuterated dimethyl sulfoxide (dimethyl sulfoxide- d_6) as solvent. The ^1H NMR spectrum obtained in this analysis was then compared with the ^1H NMR of the control sample (pure PMMA and PANi), respectively.

The transmittance and absorbance measurement of PMMA/PANi copolymer films were evaluated using Perkin Elmer Lambda 35 UV-Visible spectrophotometer. Analysis was done in the wavelength range between 300 and 900 nm with 1.0 nm sampling intervals. The sample for this analysis was spin-coated films on a glass substrate and used in the sample position while non-coated glass substrate was used in the reference position. The transmittance of spin-coated PMMA/PANi films was then compared with the spin-coated pure PMMA.

FESEM was used to visualize the morphology, agglomeration tendency, and size distribution of PMMA and PANi copolymer synthesized. This analysis was done using FESEM Jeol JSM-7600F) with a magnification of 60,000 \times at an acceleration voltage of ~5 kV. The test samples used were thin rectangular films with a dimension of 2 \times 1 cm.

2.5. Conductivity Analysis

Resistance of PMMA/PANi copolymer produced was measured by two-point probe measurement using 4200-SCS's Keithley Interactive Test Environment (KITE) source meter. The sample used for this measurement was in the form of a thin rectangular film with a dimension of 0.02 \times 0.01 m and a thickness of 8 \times 10 $^{-5}$ m. Meanwhile, the length of the needle probe was 0.005 m and fixed for every measurement of all samples. The resistivity determination was repeated five times for each sample to evaluate the accuracy.

The resistivity of PMMA/PANi copolymer was obtained using Equation (1):

$$\rho = \frac{RA}{l} (\Omega \cdot \text{m}) \quad (1)$$

where, R is the resistance of the material, A is the cross-sectional area (width, w times thickness, t), and l is the needle's length.

The conductivity of the material is simply the inverse of resistivity. It is denoted by the symbol σ and the unit of conductivity is S/m. From the resistivity value measured previously, the conductivity of PMMA/PANi copolymer was calculated using Equation (2):

$$\sigma = \frac{1}{\rho} \left(\text{S} \cdot \text{m}^{-1} \right), \quad (2)$$

3. Results

3.1. FTIR Characterization

The chemical structure of the synthesized PMMA/PANi copolymers was studied using FTIR spectroscopy. Figure 1 shows the FTIR spectra for pure PMMA and PANi, while Figure 2 shows FTIR spectra of PMMA/PANi copolymer at different polymerization times. The typical bands corresponding to the PMMA can be seen in the PMMA spectrum and listed as asymmetrical elongation vibrations of the methylene group, C-H (2953 and 2993 cm^{-1}), C=O stretching vibration (1720 cm^{-1}), CH_3 stretching (1480 and 1433 cm^{-1}), C-O-C stretching vibration (1236 cm^{-1}), -O- CH_3 stretching (1143 cm^{-1}), and $(\text{CH}_2)_n$ with $n \geq 4$ (alkene) (749 to 988 cm^{-1}) [21–23]. On the other hand, the band characteristics of PANi that can be observed in the PANi spectrum were attributed to -N-H stretching (3433 cm^{-1}), C-N stretching vibration in aromatic primary amine (1275 cm^{-1}), and ortho and meta substitution in benzene ring (732 and 684 cm^{-1}) [22,24]. In addition, peak characteristics that are responsible for conductivity can be seen at 1590 and 1593 cm^{-1} , which were attributed to stretching vibrations of quinoid and benzenoid rings, respectively [25].

FTIR spectra of PMMA/PANi 1, PMMA/PANi 2, and PMMA/PANi 3 that analyzed in the wavenumber range of 4000 to 600 cm^{-1} are shown in Figure 2. In general, all PMMA/PANi copolymer synthesized exhibited broad peaks at around 2000 to 2500 cm^{-1} wavenumber, indicating the typical form of conducting state of PANi. This broadband indicates the absorption of free charge carriers in the protonated PANi [26]. The IR bands at 1590 and 1493 cm^{-1} are attributed to C=C stretching vibrations of quinoid and benzoid rings, which are the characteristics of protonated PANi. As can be observed, these peaks were shifted to 1485 and 1583 cm^{-1} (PMMA/PANi 1), 1483 and 1584 cm^{-1} (PMMA/PANi 2) and 1483 and 1586 cm^{-1} (PMMA/PANi 3), respectively. The shifting of these peaks to lower frequency suggests the Van der Waals type of interactions or hydrogen bonding that occurred between the introduced PANi chain and PMMA matrix structure [22]. Meanwhile, the characteristic bands of emeraldine salts formed due to the protonated process of PANi with HCl can be found at bands from 1050 and 1154 cm^{-1} . Through the HCl doping process, an excitation band for emeraldine salt is formed and hence responsible for improving conductivity in PANi [27]. The intensity of the protonated bands may give an estimation of their ratio in the polymeric layer. As can be observed in IR spectra, these protonated bands are more significant for PMMA/PANi 1 and PMMA/PANi 2 spectrum as compared to PMMA/PANi 3 spectrum. Besides, the intensities of these bands are different for all the copolymer films, suggesting that these conduction bands are forming in approximately different proportions in the copolymer. As can be seen in FTIR spectrum of PMMA/PANi 1 and PMMA/PANi 2, IR band characteristics to quinoid and benzoid and emeraldine salt form of PANi are higher for PMMA/PANi 2 than those of PMMA/PANi 1, suggesting the relationship between the formation of PANi bonding with the polymerization time. These results are related to the higher proportion of PANi units in the copolymer by increasing polymerization time, which results in high conductivity, and hence in agreement with the data presented in the conductivity analysis.

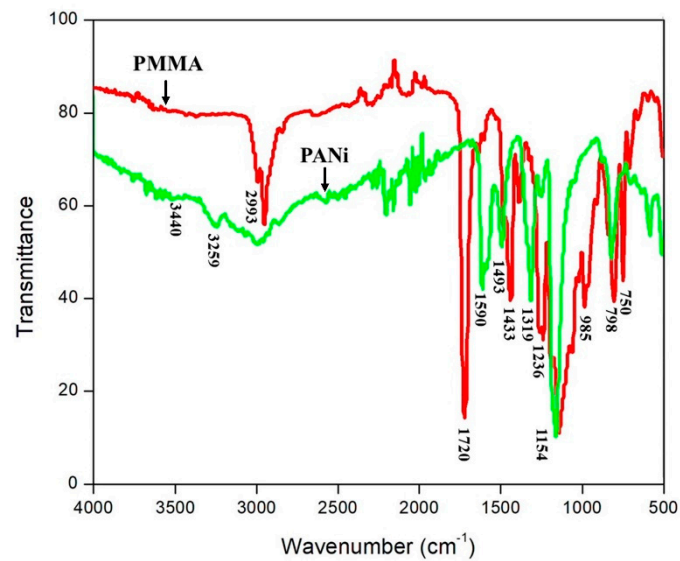


Figure 1. FTIR spectra of pure PMMA and pure PANi.

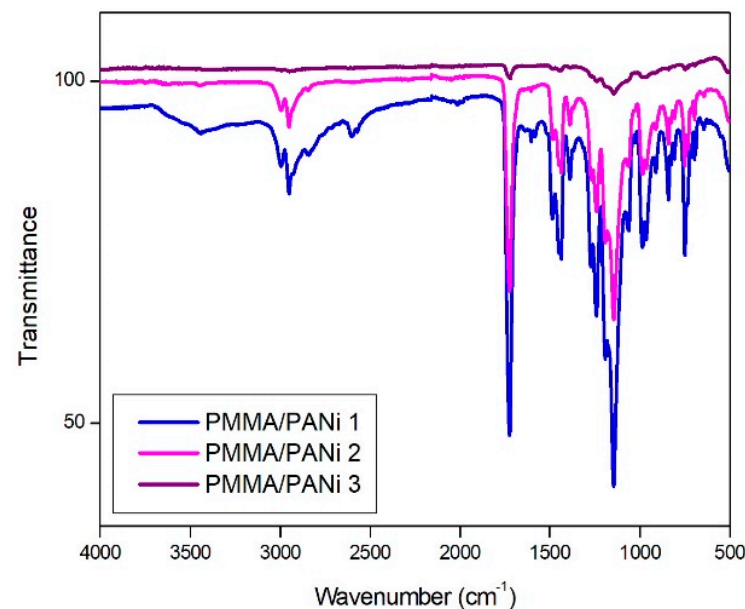


Figure 2. FTIR spectra of PMMA/PANi copolymer at different polymerization times.

The relationship between PANi proportion units in the copolymer with polymerization time can be explained in more detail with polymer conversion. It is observable that FTIR spectra of PMMA/PANi 1, PMMA/PANi 2, and PMMA/PANi 3 exhibited almost identical peaks. However, compared to PMMA/PANi 1 and PMMA/PANi 2, FTIR spectra for PMMA/PANi 3 were less apparent. The reason for this difference can be attributed to the monomer conversions which have reached a limiting conversion [28]. In the case of the free radical polymerization reaction, too long polymerization time might increase the chance of hydrogen abstraction reaction from the solvent occurring. This can happen when the radical from the propagating polymer chain end is transferred to the solvent molecules and hence reduces the polymer conversion and shortens the propagating chain [29]. The results suggest that, in free radical polymerization, more monomers are consumed by the reactive propagation chains. The slight increase in the intensities of PANi segments of the PMMA/PANi 2 spectrum indicates that polymerization at a relatively short polymerization time is favorable in regard to producing optimum PANi conversion. However, too long polymerization time (3 h) causes the reacting MMA propagating chains

to undergo a combination termination, leading to the self-polymerized PMMA [30]. The formation of the self-polymerized PMMA is unfavorable owing to the less interaction with PANi segments, which leads to the absence of few PANi characteristics band in the PMMA/PANi 3 spectrum.

It can be seen that some of the peaks had shifted to either higher or lower frequency as compared to the individual spectra of PMMA and PANi. The peak at 1433 cm^{-1} , which is attributed to C-CH₃ stretching, was shifted to higher frequency of 1448 cm^{-1} in all PMMA/PANi spectra. The peak at 798 cm^{-1} , which is attributed to C-H₂ stretching vibration, was shifted to 810 cm^{-1} for PMMA/PANi 1 and PMMA/PANi 2 and 809 cm^{-1} for PMMA/PANi 3, respectively. Meanwhile, in the case of functional groups corresponding to PANi, the peak attributed to N stretching band of aromatic amine was shifted from 1419 to 1485 cm^{-1} for PMMA/PANi 1 and 1483 cm^{-1} for PMMA/PANi 2 and PMMA/PANi 3, respectively. The shifting of peaks to higher frequency indicates that interactions took place between the hydrogen atoms of PMMA and the aromatic amines of PANi [13]. The obtained FTIR spectrum of PMMA/PANi 1 and PMMA/PANi 2 suggested that PMMA and PANi components were compatible, and an interaction existed between them. In addition, the shifting of band attributed to ring stretching for quinoid (1493 cm^{-1}) and benzenoid (1590 cm^{-1}) peak characteristics to lower frequency suggests the Van der Waals type of interactions or hydrogen bonding that occurred between the introduced PANi chain and PMMA matrix structure [31].

3.2. NMR Spectroscopy

The synthesized PMMA/PANi copolymer was further characterized by means of ¹H NMR spectroscopy. The ¹H NMR spectra of the PMMA are shown in Figure 3a, while the ¹H NMR spectra for PMMA/PANi copolymer polymerized at different polymerization times are shown in Figure 3b. For PMMA spectrum, the characteristic peaks at corresponding chemical shifts are listed as 0.7, 1.9, and 3.6 ppm, which can be assigned as CH₃, CH₂, and O-CH₃, respectively [32,33].

As depicted in Figure 3b, after copolymerization of PANi with PMMA, two new peaks that appeared at 2.3–2.4 and 6.9–7.7 ppm correspond to the N-H₂ and aromatic protons of the phenylamines groups, respectively [32]. Thus, the data obtained from ¹H NMR spectrum clearly indicate the successful copolymerization of MMA and aniline through free radical polymerization reaction.

From the ¹H NMR, it can be seen that both PMMA and PANi peaks give rise to intensity with the increases in polymerization time. The difference in intensity indicates the polymer formation for each polymerization time is different. The intensity of PANi peak signals in PMMA/PANi 2 is the highest, as the formation of PANi segment in the copolymer chain is increased during the polymerization reaction. Thus, it can be concluded that the intensity of PANi peaks for PMMA/PANi 1 is the lowest due to the least number of PANi formations in the copolymer chain. It is also found that the methylene (-CH₂) peak signal at 1.3 ppm chemical shifts is broader for PMMA/PANi 2 and PMMA/PANi 3 than that of PMMA/PANi 1. This is because the monomer incorporation into the polymer chain at longer polymerization time is higher [34].

3.3. UV-Visible Spectroscopy

The optical properties of the synthesized PMMA/PANi copolymer film were acquired using UV-Vis spectroscopy. Figure 4a shows the transmittance spectra variations of PMMA/PANi copolymer synthesized at various polymerization times and the pure PMMA thin film. According to the PMMA spectrum, it is clearly seen that, from wavelength 350 to 370 nm, there is an increase in transmittance from 0 to 94%. Then, at 370, the transmittance reduces to 85% before showing a steep increment above 100% at wavenumber 370 to 800 nm.

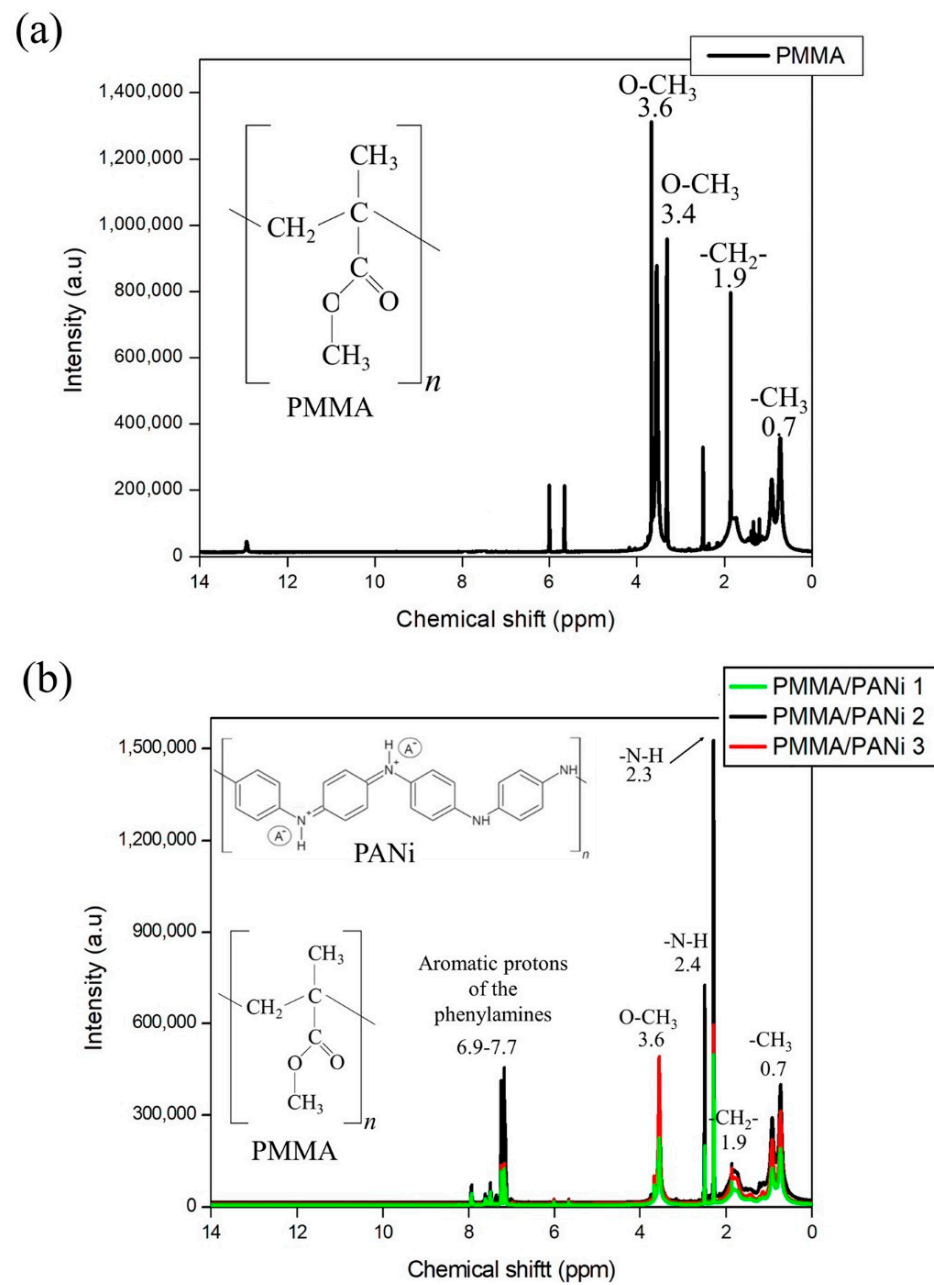


Figure 3. (a) ¹H NMR spectra of PMMA. (b) ¹H NMR spectra of PMMA/PANi copolymer polymerized at different polymerization time.

It is clearly seen that PMMA/PANi copolymer films have less transmittance than those of PMMA. For instance, the transmittance of PMMA/PANi copolymer polymerized at 3 h polymerization time (PMMA/PANi 3) exhibited the lowest transmittance (8%), followed by PMMA/PANi copolymer polymerized at 2 h polymerization time (PMMA/PANi 2), which is about 13% and 17% transmittance of PMMA/PANi copolymer polymerized at 1 h polymerization time (PMMA/PANi 1). The influence of the polymerization time (1, 2, and 3 h) on the transmittance of PMMA/PANi copolymer is not significant. For instance, the transmittance of PMMA/PANi copolymers did not differ much between one another. The flat curve between PMMA/PANi spectra is due to the dark green color of protonated PANi with HCl [35].

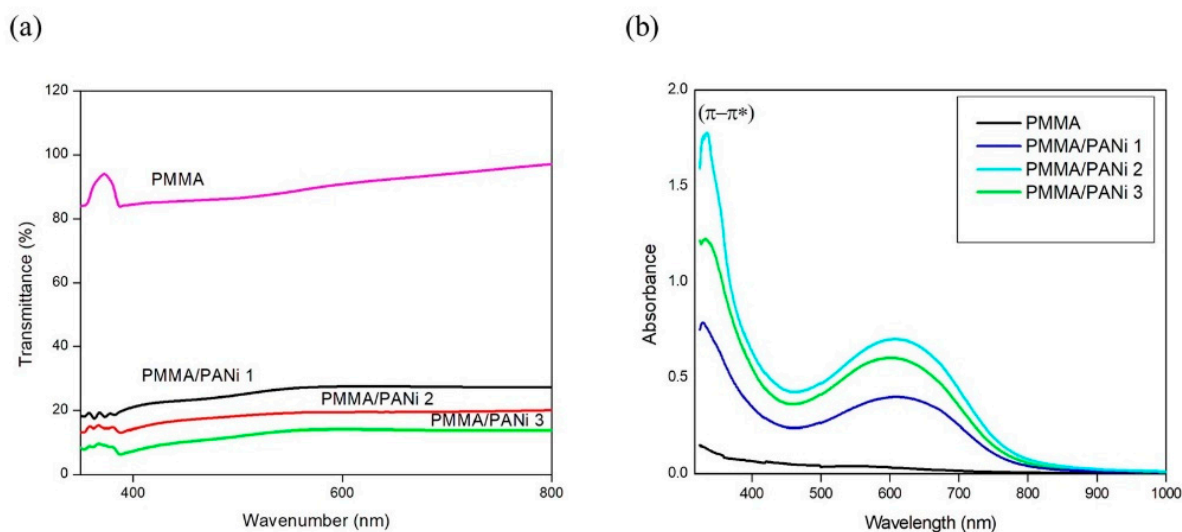


Figure 4. (a) Transmittance spectra and (b) absorbance of the PMMA and PMMA/PANi copolymer film variation with the wavelength for different polymerization times.

Meanwhile, the absorbance spectra of PMMA, and PMMA/PANi copolymers polymerized at different polymerization time (1 h, 2 h, and 3 h) are shown in Figure 4b. The spectra of PMMA/PANi copolymer show the two main absorption peaks at 328–334 nm and 553–680 nm. The first peak is attributed to $\pi-\pi^*$ transitions in the benzene ring that relates to the extent of conjugation between adjacent rings in the polymer chain [36]. Another strong broad peak is attributed to exciton formation in the quinoid ring of PANi. Thus, the presence of these two peaks in the PMMA/PANi copolymers spectrum proves the successful formation of PANi segments with alternating benzenoid and quinoid segments in the copolymer chain. It is obviously seen that the intensities of both main absorption peaks increase with increasing polymerization time from 1 h to 2 h. This may be due to the strong interaction between PANi segment or increase in the conjugated unsaturated bonds in the copolymer chains [24] with the increase in polymerization time. It is found that, the intensity of the bands is slightly reduced for PMMA/PANi 3 sample, which is in agreement with the results obtained from FTIR results in which too long polymerization time reduces the formation of PANi due to less interaction of PANi with PMMA.

3.4. Morphological Analysis

Figure 5 shows the surface images related to PMMA and PMMA/PANi copolymer. All of the PMMA/PANi copolymer films show a coral-like morphology that consists of branched PANi nanofibers. The obtained PANi microstructures are the common HCl-doped PANi microstructures obtained from chemical oxidation polymerization reaction [37]. The diameter of most of the PMMA/PANi copolymer obtained here was ≈ 30 nm.

Obviously, there is a significant difference in the copolymer surfaces with the variation of polymerization time. The formation of PANi on PMMA matrix is found to be time-dependent. PANi that had been formed by 1-h and 2-h polymerization time exhibited a highly defined and porous structure. In general, at 2-h polymerization time, newly polymerized PANi molecules would grow from previously constructed PANi structures because PANi structures that were already formed previously become dominant, despite prolonging the polymerization time. However, when the polymerization time was further increased more than the optimized polymerization time (3-h), the PANi structures became agglomerated due to excessive generation of PANi, causing the microstructures to lose their shape and definition [38].

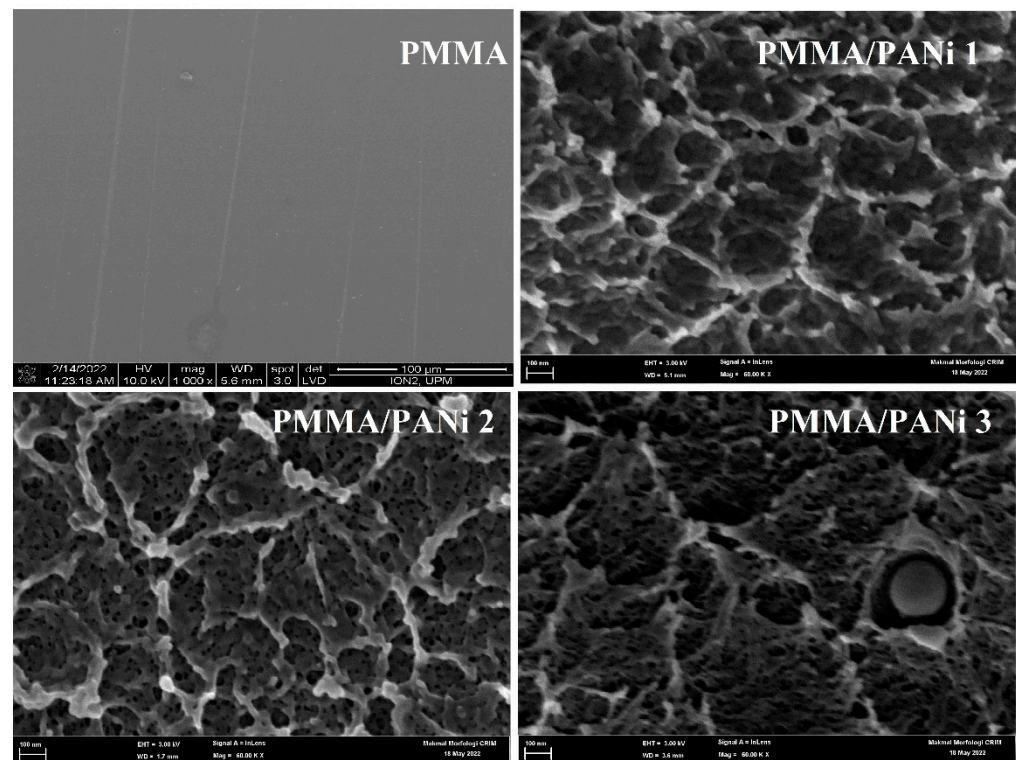


Figure 5. FESEM images of PMMA and PMMA/PANi polymerized at various polymerization times at 60,000 \times magnification.

3.5. Conductivity Measurement

Figure 6 shows the I–V curve of PMMA and PMMA/PANi copolymer measured by the 2-probe method. Using Equations (1) and (2), the conductivity of all samples was calculated and tabulated in Table 1. Based on the conductivity calculated, PANi has a great influence on the conductivity of PMMA. The conductivity of the film is due to the presence of quinoid and benzenoid ring in PANi structure that facilitates the movement of electrons around the copolymer chain [25,39].

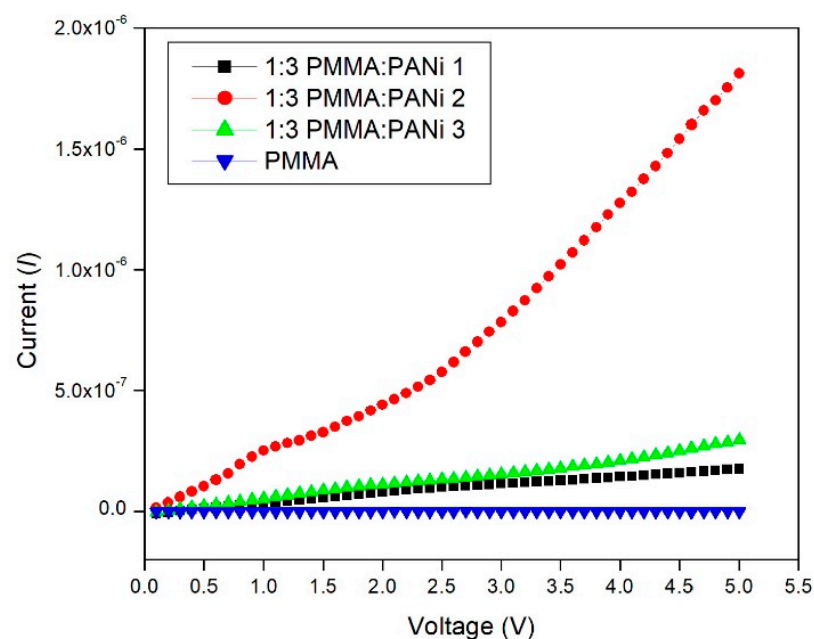


Figure 6. Relationship between current and voltage of PMMA and PMMA/PANi copolymer films.

Table 1. Conductivity calculated for PMMA and PMMA/PANi copolymer.

Sample	Polymerization Time (h)	Conductivity (S/m)
PMMA	-	3.61×10^{-9}
PMMA/PANi 1	1	7.76×10^{-5}
PMMA/PANi 2	2	2.34×10^{-4}
PMMA/PANi 3	3	8.28×10^{-5}

In addition, it is found that there are differences in conductivity values for the various polymerization times used. The highest conductivity value was recorded for PMMA/PANi 2 copolymer film (2.34×10^{-4} S/m). This suggests the optimum polymerization time for PMMA/PANi copolymerization, which is at 2 h. The calculated conductivity also substantiates that increased polymerization time would increase the conductivity of PANi until it reaches optimum polymerization time. This result is in line with the results obtained from FTIR and FESEM where an increased polymerization time improves the formation of PANi as compared to short polymerization time (1 h), indicating well conversion of aniline monomer. The increase of conductivity with polymerization time is said to be due to an increase in crystallinity and molecular weight as PANi grows [19]. Nevertheless, too long polymerization time reduces conductivity of PMMA/PANi copolymer because the copolymer chain reached the optimum formation, and excess PANi formation caused agglomeration of PANi.

4. Conclusions

PMMA/PANi copolymer by free radical polymerization reaction was successfully synthesized. This is proven by FTIR and ^1H NMR spectra that identified the presence of peak characteristics and chemical shifts of PMMA together with benzenoid and quinoid structures attributed to PANi. In this work, we report the influence of different polymerization times on the properties of PMMA/PANi copolymer. Analysis using FTIR indicated that PMMA/PANi copolymer polymerized at longer polymerization time shows less significant peaks, suggesting that monomer conversion increases with time until it reaches limited conversion. The ^1H NMR spectra of PMMA and PMMA/PANi copolymer suggested successful copolymerization of PMMA with PANi with copolymerization at higher polymerization time gives higher polymer formation. According to the UV-Vis spectroscopy results, PMMA/PANi spectra showed distinct differences in percent transmittance as compared to PMMA. In addition, prolonged polymerization time is found to reduce the transmittance of PMMA/PANi copolymer due to the dark green color of protonated PANi with HCl. The absorbance spectra of the copolymers are in agreement with the results obtained in both FTIR and ^1H NMR analysis, where the formation of PANi segment in the copolymer chain depends on the polymerization time. Morphological study using FESEM showed nanofibers polyaniline with increased polymerization time. Conductivity measurement using the 2-probe method has shown that the conductivity of PMMA/PANi polymerized at this optimum polymerization time exhibited the highest conductivity of 2.34×10^{-4} S/m. Overall, this study reinforces the effect of polymerization time on fabricating conducting PMMA by copolymerization with PANi. In the near future, the suitability of conducting PMMA/PANi to be used in many electronic devices can be further explored.

Author Contributions: Conceptualization, H.A.H.S. and M.M.R.; investigation, H.A.H.S., M.M.R., M.N.M., N.A.R., F.R. and A.A.; resources, H.A.H.S., M.M.R., M.M.A.B.A., F.R. and M.N.M.; data curation, H.A.H.S., M.M.R., M.N.M., N.A.R., M.M.A.B.A., N.H.O., F.R. and A.A.; writing—original draft preparation, H.A.H.S., M.M.R. and M.N.M.; writing—review and editing, H.A.H.S., M.M.R., M.N.M. and N.H.O.; supervision, M.M.R. and M.N.M.; funding acquisition, M.M.R., M.M.A.B.A. and M.N.M. All authors have read and agreed to the published version of the manuscript.

Funding: This research was supported by Universiti Putra Malaysia Research Grant (GP-IPB/2017/9563800).

Institutional Review Board Statement: Not applicable.

Informed Consent Statement: Not applicable.

Data Availability Statement: The data presented in this study are available on request from the corresponding author.

Conflicts of Interest: The authors declare no conflict of interest.

References

1. Shirakawa, H.; Louis, E.J.; MacDiarmid, A.G.; Chiang, C.K.; Heeger, A.J. Synthesis of electrically conducting organic polymers: Halogen derivatives of polyacetylene, (CH)_x. *J. Chem. Soc. Chem. Commun.* **1977**, 578–580. [[CrossRef](#)]
2. Li, Z.; Gong, L. Research progress on applications of polyaniline (PANI) for electrochemical energy storage and conversion. *Materials* **2020**, *13*, 548. [[CrossRef](#)] [[PubMed](#)]
3. Gholami Laelabadi, K.; Moradian, R.; Manouchehri, I. One-Step Fabrication of Flexible, Cost/Time Effective, and High Energy Storage Reduced Graphene Oxide@PANI Supercapacitor. *ACS Appl. Energy Mater.* **2020**, *3*, 5301–5312. [[CrossRef](#)]
4. Rong, G.; Zhou, D.; Pang, J. Preparation of high-performance antifouling polyphenylsulfone ultrafiltration membrane by the addition of sulfonated polyaniline. *J. Polym. Res.* **2018**, *25*, 66. [[CrossRef](#)]
5. Qiang, Z.; Liang, G.; Gu, A.; Yuan, L. The dielectric behavior and origin of high-k composites with very low percolation threshold based on unique multi-branched polyaniline/carbon nanotube hybrids and epoxy resin. *Compos. Part A Appl. Sci. Manuf.* **2014**, *64*, 1–10. [[CrossRef](#)]
6. Biswas, S.; Jeong, H.-S.; Jeong, J.-B.; Cho, B.; Lee, S.; Lee, D.-W.; Lang, P.; Bae, J.-H.; Kim, H. Synthesis and Charge Transport of Polymer Nanocomposite of Polyaniline: Polystyrene Sulfonate. *J. Nanosci. Nanotechnol.* **2019**, *19*, 4638–4642. [[CrossRef](#)]
7. Bandeira, R.M.; Bezerra Amorim, D.R.; Vega, M.L.; Elias de Matos, J.M.; Ribeiro dos Santos Júnior, J.; Nunes da Cunha, H. Charge transport in benzoic acid-doped polyaniline films. *Mater. Chem. Phys.* **2021**, *260*, 124083. [[CrossRef](#)]
8. Bhadra, J.; Al-Thani, N.J.; Madi, N.K.; Al-Maadeed, M.A. Effects of aniline concentrations on the electrical and mechanical properties of polyaniline polyvinyl alcohol blends. *Arab. J. Chem.* **2017**, *10*, 664–672. [[CrossRef](#)]
9. Abutalib, M.M. Insights into the structural, optical, thermal, dielectric, and electrical pr1. Abutalib, M.M. Insights into the structural, optical, thermal, dielectric, and electrical properties of PMMA/PANI loaded with graphene oxide nanoparticles. *Phys. B Condens. Matter* **2019**, *52*, 19–29. [[CrossRef](#)]
10. Sahu, S.; Sahoo, A.P.; Shubhadarshinee, L.; Ramakrishna, D.S.; Barick, A.K. Effect of polyaniline-coated carbon nanotube and nanosilver hybrid nanoparticles on the dielectric properties of poly(methyl methacrylate) nanocomposites. *Polym. Compos.* **2018**, *39*, E1294–E1305. [[CrossRef](#)]
11. Saad Ali, S.; Pauly, A.; Brunet, J.; Varenne, C.; Ndiaye, A.L. MWCNTs/PMMA/PS composites functionalized PANI: Electrical characterization and sensing performance for ammonia detection in a humid environment. *Sens. Actuators B Chem.* **2020**, *320*, 128364. [[CrossRef](#)]
12. Wang, W.; Narain, R.; Zeng, H. Chapter 10-Hydrogels. In *Polymer Science and Nanotechnology*; Narain, R., Ed.; Elsevier: Amsterdam, The Netherlands, 2020; pp. 203–244, ISBN 978-0-12-816806-6.
13. Mishra, S.; Ghodki, N. Synthesis and Characterization of a Novel Conducting Biopolymer Chitosan Grafted Polyaniline-Polypyrrole Flexible Copolymer Battery View project Development of Polymer/MWCNT nano-composites for Mechanical and Tribological Applications View project Synthes. *Int. J. Sci. Res. Methodol.* **2017**, *1*.
14. Li, X.G.; Zhou, H.J.; Huang, M.R. Synthesis and properties of processable conducting copolymers from N-ethylaniline with aniline. *J. Polym. Sci. Part A Polym. Chem.* **2004**, *42*, 6109–6124. [[CrossRef](#)]
15. Amorim, D.R.B.; da Silva Guimarães, I.; Fugikawa-Santos, L.; Vega, M.L.; da Cunha, H.N. Effect of temperature on the electrical conductivity of polyaniline/cashew gum blends. *Mater. Chem. Phys.* **2020**, *253*, 123383. [[CrossRef](#)]
16. Noby, H.; El-Shazly, A.H.; Elkady, M.F.; Ohshima, M. Strong acid doping for the preparation of conductive polyaniline nanoflowers, nanotubes, and nanofibers. *Polymer* **2019**, *182*, 121848. [[CrossRef](#)]
17. Wu, R.; Yuan, H.; Liu, C.; Lan, J.-L.; Yang, X.; Lin, Y.H. Flexible PANI/SWCNT thermoelectric films with ultrahigh electrical conductivity. *RSC Adv.* **2018**, *8*, 26011–26019. [[CrossRef](#)]
18. Sanches, E.A.; Soares, J.C.; Mafud, A.C.; Fernandes, E.G.R.; Leite, F.L.; Mascarenhas, Y.P. Structural characterization of Chloride Salt of conducting polyaniline obtained by XRD, SAXD, SAXS and SEM. *J. Mol. Struct.* **2013**, *1036*, 121–126. [[CrossRef](#)]
19. Maity, P.C.; Khandelwal, M. Synthesis time and temperature effect on polyaniline morphology and conductivity. *Am. J. Mater. Synth. Process.* **2016**, *1*, 37–42. [[CrossRef](#)]
20. Mazzeu, M.A.C.; Faria, L.K.; Baldan, M.R.; Rezende, M.C.; Gonçalves, E.S. Influence of reaction time on the structure of polyaniline synthesized on a pre-pilot scale. *Braz. J. Chem. Eng.* **2018**, *35*, 123–130. [[CrossRef](#)]
21. Duan, G.; Zhang, C.; Li, A.; Yang, X.; Lu, L.; Wang, X. Preparation and characterization of mesoporous zirconia made by using a poly (methyl methacrylate) template. *Nanoscale Res. Lett.* **2008**, *3*, 118–122. [[CrossRef](#)]
22. Ghorbel, E.; Hadriche, I.; Casalino, G.; Masmoudi, N. Characterization of thermo-mechanical and fracture behaviors of thermo-plastic polymers. *Materials* **2014**, *7*, 375–398. [[CrossRef](#)] [[PubMed](#)]

23. Hamlaoui, F.Z.; Naar, N. Improvement of the structural and electrical properties of PMMA/PANI-MA blends synthesized by interfacial in situ polymerization in a continuous organic phase. *Polym. Bull.* **2020**, *79*, 37–63. [[CrossRef](#)]
24. Khan, M.D.A.; Akhtar, A.; Nabi, S.A. Investigation of the electrical conductivity and optical property of polyaniline-based nanocomposite and its application as an ethanol vapor sensor. *New J. Chem.* **2015**, *39*, 3728–3735. [[CrossRef](#)]
25. Waware, U.S.; Hamouda, A.M.S.; Majumdar, D. Synthesis, characterization and physicochemical studies of copolymers of aniline and 3-nitroaniline. *Polym. Bull.* **2020**, *77*, 4469–4488. [[CrossRef](#)]
26. Trchová, M.; Stejskal, J. Polyaniline: The infrared spectroscopy of conducting polymer nanotubes (IUPAC Technical report). *Pure Appl. Chem.* **2011**, *83*, 1803–1817. [[CrossRef](#)]
27. Butoi, B.; Groza, A.; Dinca, P.; Balan, A.; Barna, V. Morphological and structural analysis of polyaniline and poly(o-anisidine) layers generated in a DC glow discharge plasma by using an oblique angle electrode deposition configuration. *Polymers* **2017**, *9*, 732. [[CrossRef](#)] [[PubMed](#)]
28. Pladis, P.; Karidi, K.; Meimaroglou, D.; Kiparissides, C. A Comprehensive Kinetic Investigation of the Ring Opening of L,L-Lactide in the Presence of Multifunctional Polyalcohols. In *26th European Symposium on Computer Aided Process Engineering; Kravanja, Z., Bogataj, M., Eds.; Computer Aided Chemical Engineering; Elsevier: Amsterdam, The Netherlands, 2016; Volume 38*, pp. 1153–1158.
29. Hocking, M.B. Addition (Chain Reaction) Polymer Theory. *Handb. Chem. Technol. Pollut. Control* **2005**, 713–736. [[CrossRef](#)]
30. Kongkaew, A.; Wootthikanokkhan, J. Effects of reaction conditions on poly(methyl methacrylate) polymerized by living radical polymerization with iniferter. *J. Appl. Polym. Sci.* **2000**, *75*, 938–944. [[CrossRef](#)]
31. Kowalczyk, D.; Pitucha, M. Application of FTIR method for the assessment of immobilization of active substances in the matrix of biomedical materials. *Materials* **2019**, *12*, 2972. [[CrossRef](#)]
32. Massoumi, B.; Mozaffari, Z. Synthesis and properties of electroactive polyaniline-graft-poly(2-hydroxy ethyl methacrylate) copolymers. *Polym. Sci.-Ser. B* **2014**, *56*, 369–376. [[CrossRef](#)]
33. Abdelkader, R.; Amine, H.; Mohammed, B. H-NMR Spectra of Conductive, Anticorrosive and Soluble Polyaniline 1 Exchanged by an Eco-Catalyst Layered (Maghnite-H). *World J. Chem.* **2013**, *8*, 20–26. [[CrossRef](#)]
34. Perrier, S.; Haddleton, D.M. In Situ NMR Monitoring of Living Radical Polymerization. *Situ Spectrosc. Monomer Polym. Synth.* **2003**, 125–146. [[CrossRef](#)]
35. Jum'ah, I.; Mousa, M.S.; Mhawish, M.; Sbeih, S.; Telfah, A. Optical and structural properties of (PANI-CSA-PMMA)/NiNPs nanocomposites thin films for organic optical filters. *J. Appl. Polym. Sci.* **2020**, *137*, 48643. [[CrossRef](#)]
36. Abdul Rahman, N.; Gizdavic-Nikolaidis, M.; Ray, S.; Easteal, A.J.; Travas-Sejdic, J. Functional electrospun nanofibres of poly(lactic acid) blends with polyaniline or poly(aniline-co-benzoic acid). *Synth. Met.* **2010**, *160*, 2015–2022. [[CrossRef](#)]
37. Mo, Y.; Meng, W.; Xia, Y.; Du, X. Redox-active gel electrolyte combined with branched polyaniline nanofibers doped with ferrous ions for ultra-high-performance flexible supercapacitors. *Polymers* **2019**, *11*, 1357. [[CrossRef](#)]
38. Lee, K.; Cho, S.; Kim, M.; Kim, J.; Ryu, J.; Shin, K.Y.; Jang, J. Highly porous nanostructured polyaniline/carbon nanodots as efficient counter electrodes for Pt-free dye-sensitized solar cells. *J. Mater. Chem. A* **2015**, *3*, 19018–19026. [[CrossRef](#)]
39. Rangel-Vazquez, N.A.; Sánchez-López, C.; Rodríguez Felix, F. Spectroscopy analyses of polyurethane/polyaniline IPN using computational simulation (Amber, MM+ and PM3 method). *Polimeros* **2014**, *24*, 453–463. [[CrossRef](#)]